JACS
JOURNAL OF THE AMERICAN CHEMICAL SOCIETY

Communication

pubs.acs.org/JACS

# In Situ Live Observation of Nucleation and Dissolution of Sodium Chlorate Nanoparticles by Transmission Electron Microscopy

Yuki Kimura,*[,†] Hiromasa Niinomi,[†,§] Katsuo Tsukamoto,[†] and Juan M. García-Ruiz*[,‡]

[†]Department of Earth and Planetary Materials Science, Graduate School of Science, Tohoku University, Aramakiaza-Aoba 6-3, Aoba-ku, Sendai 980-8578, Japan

[‡]Laboratorio de Estudios Cristalográficos, Instituto Andaluz de Ciencias de la Tierra, Consejo Superior de Investigaciones Científicas−Universidad de Granada, Av. de las Palmeras 4, 18100 Granada, Spain

Supporting Information

**ABSTRACT:** The formation of crystals from solution requires the initial self-assembly of units of matter into stable periodic structures reaching a critical size. The early stages of this process , called nucleation, are very difficult to visualize. Here we describe a novel method that allows real time observation of the dynamics of nucleation and dissolution of sodium chlorate clusters in an ionic liquid solution using in situ transmission electron microscopy. Using ionic liquids as solvent circumvents the problem of evaporation and charging, while the nucleation frequency was reduced by using saturated solutions. We observe simultaneous formation and dissolution of prenucleation clusters, suggesting that high-density fluctuations leading to solid cluster formation exist even under equilibrium conditions. In situ electron diffraction patterns reveal the simultaneous formation of crystalline nuclei of two polymorphic structures, the stable cubic phase and the metastable monoclinic phase, during the earliest stages of nucleation. These results demonstrate that molecules in solution can form clusters of different polymorphic phases independently of their respective solubility.

The birth of a crystal from its mother solution is one of the most intriguing problems in solid-state physics.[1] The current view of the process was formalized during the first half of the 20th century and is based on the competition between the free energy created when molecules in the solution cluster to form a solid phase and the free energy consumed as a result of the surface creation.[2] Accordingly, the energy required to form a crystalline cluster is maximum for a particular size, called the size of the critical nucleus.[3] This view of crystal formation has recently been challenged by a "two-step" approach in which the pathway for overcoming the energy barrier can be lowered by prior formation of either dense liquid fluid or amorphous but stable clusters that might later form the crystalline nucleus.[4−8]

Testing the actual nucleation pathway experimentally at the nanoscale presents formidable challenges. Atomic force microscopy and novel techniques of transmission electron microscopy (TEM) using fluid cells have provided exquisite information on the size and structure of clusters in frozen stages at the nanoscale,[9−11] as well as a dynamic view of the growth and coalescence of nuclei.[12−14] However, a live observation of the dynamics during the earliest stages of nucleation, those taking place before the formation of a stable crystal, has never been achieved. The reason is that in situ observation of nucleation at the nanoscale using TEM faces serious difficulties, particularly those related to solvent evaporation, charge dissipation and image acquisition speed. To circumvent the problem of evaporation and charging, we have used an ionic solvent having negligible vapor pressure and relatively high electrical conductivity.[15] To overcome the problem of visualization, we have used saturated solutions, where crystalline clusters are expected either not to form or to do it at a slow rate, and will never reach a critical size, thus making the observation of the dynamics easier, cleaner and more informative.

Ionic liquids have previously been used for direct observation of organic materials, such as seaweed by scanning electron microscopy (SEM)[16] and dispersed metallic nanoparticles by TEM.[17] There are several hundreds of ionic liquids that have been categorized into several systems, such as aliphatic, imidazolium, or pyridium. We selected the following five ionic liquids (Kanto Chemical Co., Inc., Tokyo, Japan) as candidate solvents, taking into account their melting point, dissociation temperature, price, and availability. The ionic liquid must be liquid at room temperature for nucleation and must be stable, showing no dissociation during the heating experiments; 1,3-diallylimidazolium bromide, 1-allyl-3-butylimidazolium bromide, 1-ethyl-3-methylimidazolium tetrafluoroborate, 1-butyl-3-methylimidazolium tetrafluoroborate, and 1-allyl-3-ethylimidazolium bromide. The first of these ionic liquids was found the best solvent to study $NaClO_3$ nucleation. Its chemical formula weight is 229.12 and its decomposition temperature is 271 °C. Its chemical formula is $C_9H_{13}BrN_2$.

Saturated solutions of $NaClO_3$ (analytical grade, Wako Pure Chemical) in ionic solution at 80 °C were prepared as follows. $NaClO_3$ powder was poured into the ionic liquid (500 μL) and stirred using ultrasound. The solution was stored for 2 days at 85 °C, then cooled down to 80 °C and stored for 1 day. A residue of undissolved $NaClO_3$ was observed at the bottom of the ionic solution confirming that the supernatant ionic liquid solution was saturated with $NaClO_3$ at 80 °C. Saturated ionic solution of 5−10 μL was removed from the middle of the solution using a pipet previously warmed to 80 °C. The

**Received:** November 27, 2013
**Published:** January 21, 2014

ACS Publications © 2014 American Chemical Society



dx.doi.org/10.1021/ja412111f | J. Am. Chem. Soc. 2014, 136, 1762−1765

solution was then dropped onto two different types of substrates. The first one was a temperature-controlled glass substrate for observation by polarized-light optical microscopy, which allows the identification of the polymorphs of $NaClO_3$ (Figure S1). The second substrate was an amorphous carbon holey film supported on a standard copper TEM grid (Figure 1). The contrast of the solution in TEM image depends on the

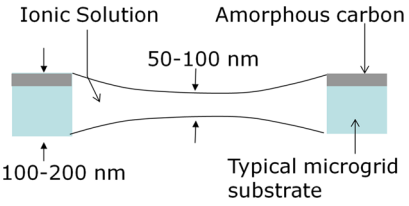


**Figure 1.** Schematic side view of the holey film on the TEM grid. The diameter of each hole is of the order of several micrometers. The ionic solution is self-supporting as a result of surface tension. The volume of the ionic liquid contained in a hole in the holey film was approximately from $10^{-19}$ to $10^{-18}$ $m^3$.

thickness of the solution. We controlled the amount of the bulk solution dropped onto the microgrid and selected a hole, which has a weaker contrast at the center compared with the periphery. Therefore, thickness of the solution is thinner than the thickness of the microgrid (100−200 nm) and can be estimated to be in the range from 50 to 100 nm.

We used two TEMs: a Hitachi H-8100 (located at the Tohoku University, Sendai, Japan) and an H-9500 (located at Hitachi High-Technologies Corporation, Ibaraki, Japan) equipped with a double-tilt heating holder. The H-8100 TEM was operated at an accelerating voltage of 200 kV and had a tungsten filament. In the initial TEM experiments, our aim was to crystallize the sodium chlorate solution in the TEM holder at room temperature. Figure 2 shows TEM micrographs of the

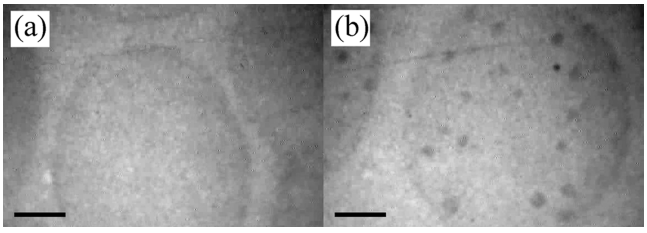


**Figure 2.** Snapshots of in situ TEM observations of $NaClO_3$ crystals at an acceleration voltage of 200 kV. (a) Starting ionic liquid solution of $NaClO_3$ saturated at 80 °C; (b) the same solution observed after 30 min at a temperature of ∼25 °C (supercooling $\Delta T$ = 55 °C). Strong contrasts in (b) show crystals of $NaClO_3$ with a diameter of 50−150 nm. The growth rate was ∼10 nm $s^{-1}$. The scale bar corresponds to 500 nm.

supersaturated solution before and after nucleation of $NaClO_3$. A stable population of crystals up to 150 nm in size can be observed. Notice that, as expected, the volume of the ionic solution remained constant throughout the entire observation period, with no signs of evaporation. This grid was then placed inside a double-tilt heating holder of a Hitachi H-9500 TEM operated at 300 kV, heated from room temperature to 60 °C, and recorded (Video S1). The temperature of the specimen slightly increases by Joule's heat, which is produced when incident electrons lose their energy by inelastic collisions. However, since the electron dose of our experiment is very low [(3.0−6.1) × $10^3$ e $nm^{-2}$ $s^{-1}$], the heating of our sample is small enough to be neglected (see SI, section S3).

As expected, the previously formed crystals start to dissolve after heating (Figure 3). Upon dissolution, the concentration of the solute in the vicinity of the crystals increases until

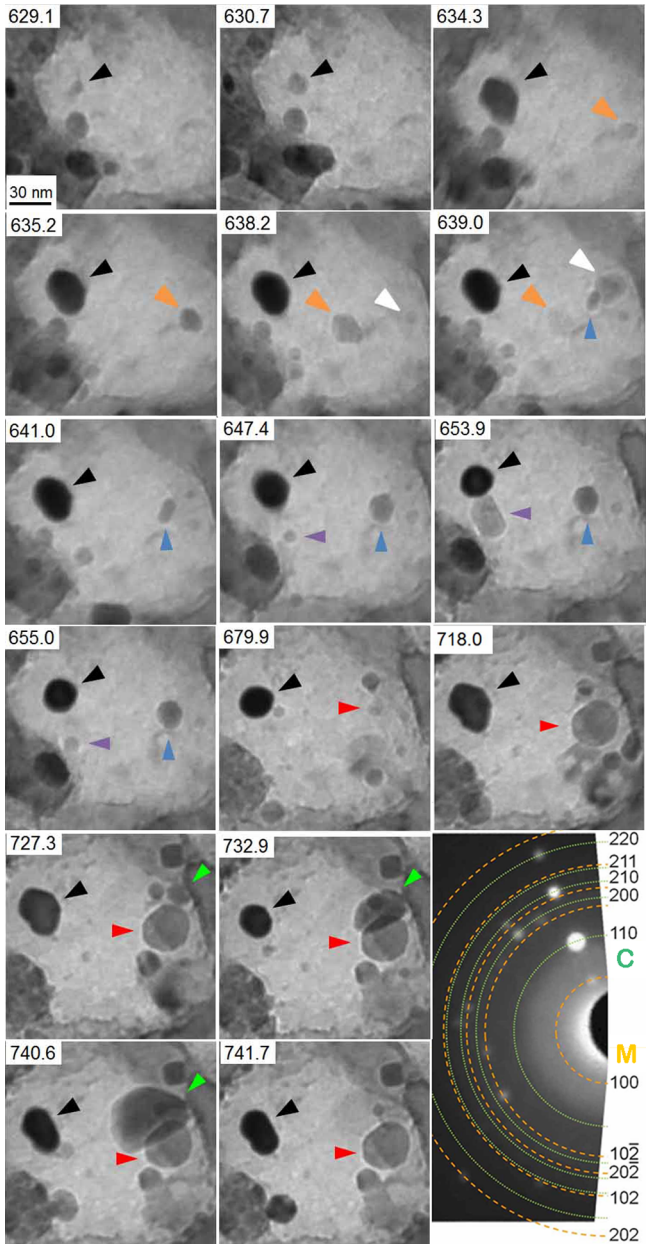


**Figure 3.** Still snapshots of in situ bright-field TEM observations at 60 °C from Video S1. The pictures are labeled with time in seconds after start to elevate temperature. The black triangles show a cubic particle that nucleates at time 626.9 s, grows, and remains stable during the observation. The orange, white, and blue triangles indicate the nucleation and dissolution of a crystal. Rounded crystal indicated by the red triangles remained stable over a prolonged period. The green triangles mark the formation and rapid dissolution of a metastable crystal. The last frame of the figure (at the right) is an electron diffraction pattern taken after visualization showing the existence of two polymorphs of $NaClO_3$ in the experiment. The solid green and broken orange lines correspond to cubic and monoclinic phases as labeled by "C" and "M", respectively, and are labeled with their respective crystal indexes.


dx.doi.org/10.1021/ja412111f | J. Am. Chem. Soc. 2014, 136, 1762−1765

saturation. According to the classical theory, no crystals are expected to form in the resulting equilibrium solution. We observed that actually they do form. As clearly shown in Video S1 and Figure 3, particles appear and disappear rapidly in the equilibrium solution surrounding the dissolving crystals, i.e., that precritical nuclei form spontaneously under conditions at equilibrium. The depth of focus in Figure 3 was estimated to be roughly 55 nm (SI, section S3), i.e., of the same order of magnitude as the thickness of the solution. In addition, none of the particles show Fresnel fringes characteristic of defocusing objects. Hence, the particles remain in focus during the observation. The thickness of the particles could not be determined, but they were certainly smaller than the thickness of the drop, estimated to be thinner than ~100 nm. Therefore, we measured the size of the particles from the area they projected on the focal plane of the microscope. An important source of error when measuring crystal size is the rotation of crystals during the observation. Rotating particles can be identified by changes in their diffraction contrast. Therefore, all data from particles that were detected rotating were not used in the analysis.

We propose that existence of these clustering processes must be triggered by local fluctuations of density. In fact, these fluctuations provoking local nanovolumes of higher concentration where precritical nuclei might form have been already observed in noncrystallizing solutions.[18] It has also been suggested that they might occur during the earliest stages of the two-step nucleation process.[13,14] We have found that the formation rate of crystalline clusters is unexpectedly high ($\sim 3 \times 10^{20}$ m$^{-3}$ s$^{-1}$), and the radial growth rates of the crystalline clusters are fast ($4.2 \pm 2.7$ nm s$^{-1}$, see Figures 4 and S3). This kinetics suggests that the amplitude of density fluctuations either reach local supersaturation values much beyond the equilibrium or have a high degree of order.

If we assume that the diffusion coefficient of $NaClO_3$ in the ionic liquid is $10^{-11}$ m$^2$ s$^{-1}$ (2 orders of magnitude lower than the diffusion coefficient in water[19]), the $NaClO_3$ molecules could travel a distance of ~600 nm during the 40 ms of the exposure time, i.e., their movement would have been too rapid to be captured by TEM. The diffusion coefficient is proportional to the diameter of the particles with the Stokes−Einstein equation. A particle with a size of approximately 50 nm is the minimum size, which diffuses a shorter distance than own particle diameter during the exposure time. Nevertheless, we see many particles smaller than 50 nm in Video S1. Those crystals can be observed because they remain at the same location of the surface of ionic liquid by surface tension. Therefore, the growth units of $NaClO_3$ transfer from the solution to the crystalline precritical nucleus or an amorphous stable precursor is not detectable in the current experimental setup. More precisely, amorphous particles either do not form or they are smaller than 50 nm, i.e., they contain fewer than $9 \times 10^4$ monomers and their lifetime is no longer than 40 ms. In addition, the rapid formation of crystalline clusters from saturated solutions and the fast growth rates both suggest that local high density or high ordered nanovolumes provoked by fluctuations play a role during classical nucleation.[20,21]

In addition to the stable cubic precritical nuclei, we also observed the metastable monoclinic phase of $NaClO_3$ identified by in situ electron diffraction patterns (Figure 3). Sodium chlorate can crystallize from solution in two different crystal structures:[22] a thermodynamically stable cubic (space group, *P*213; lattice constant, $a$ = 6.5756 Å) and a metastable monoclinic phase of higher solubility [$P21/a$, $a$ = 8.42(2), $b$ = 5.260(7), $c$ = 6.70(1) Å and $\beta$ = 109.71(1)°]. The lifetime of the monoclinic nuclei is shorter than that of the cubic ones, as shown by the blue and green triangles in Figure 3. It is also clear that, whereas the growth rates of the stable crystals are similar ($4.2 \pm 2.8$ nm s$^{-1}$) to the metastable crystals ($3.6 \pm 1.1$ nm s$^{-1}$), the dissolution rate of the metastable crystals ($12.6 \pm 5.4$ nm s$^{-1}$) is faster than that of the stable crystals ($7.6 \pm 6.1$ nm s$^{-1}$). Thus, the solubility of the metastable monoclinic phase can be inferred to be higher than the solubility of the cubic phase for the whole range of temperature of the experiment. Ostwald "law" of stages states that the precipitation sequence of polymorphs starts with the less stable phase and ends with the more stable one.[23] Our results demonstrate that prenucleation clusters of different polymorphs form simultaneously independently of their respective solubility values. The arrangement of the molecules or ions arising from a maximal local concentration seems to be merely the result of a compromise between the disorder of the accumulation, i.e., the rate at which molecules or ions cluster in a single location, and the degree of structural order of the different polymorphic configurations.[24] The lifetime of the nuclei with different structural arrangements depends on their individual surface energy and its variation with size,[25] thus explaining the exclusive detection of the cubic phase at micrometer or larger scale.

The formation of polymorphs simultaneously at the earliest stages of nucleation is a plausible explanation for the formation of metastable phases as precursors well below the equilibrium solubility.[9] In addition, our technique can be used as an efficient screening method for the search of polymorphic phases, as this technique allows us to identify formation of clusters of different

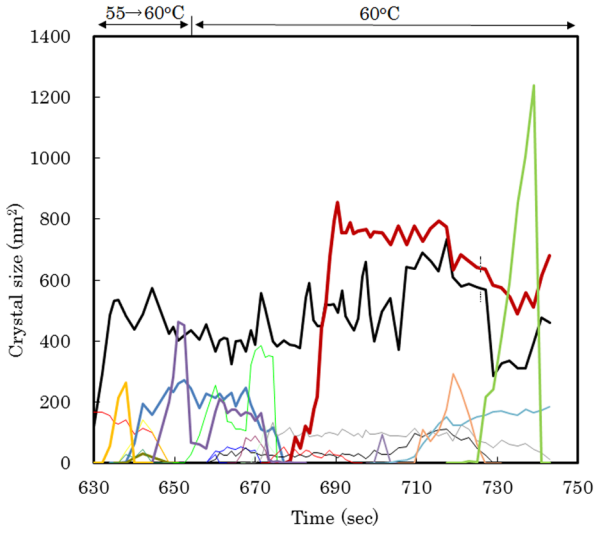


**Figure 4.** Time evolution of particle size. The size was measured from the surfaces of their projected areas on the focal plane of the TEM. Each line is marked with the same colors and symbols used in Figure 3. Note that some of the crystals fluctuate in size. A most noticeable phenomenon is that crystal dissolution did not occur smoothly by continuous loss of mass. The frame sequence shown in Video S1 dynamically illustrates that both the shape and size of the particle vary with time, showing episodes of growth and dissolution. The amplitude of these size fluctuations is sometimes as large as 20 nm. Growth and dissolution rates calculated from these data are plotted in Figure S4.


dx.doi.org/10.1021/ja412111f | J. Am. Chem. Soc. 2014, 136, 1762−1765

polymorphs before the less stable phases disappear as a result of surface energy competition.

## ■ ASSOCIATED CONTENT

### Supporting Information

Supporting video, optical microscopy studies, in situ observation by TEM, direct observation of the Ostwald's ripening, histograms of the growth and dissolution rates and variations in the growth and dissolution rates. This material is available free of charge via the Internet at http://pubs.acs.org.

## ■ AUTHOR INFORMATION


### Corresponding Authors

ykimura@m.tohoku.ac.jp
jmgruiz@ugr.es

### Present Address

[§]H.N.: Department of Materials Science and Engineering, Nagoya University, Furo-cho, Chikusa, Nagoya 464−8603, Japan.


### Notes

The authors declare no competing financial interest.

## ■ ACKNOWLEDGMENTS

We thank H. Matsumoto, Y. Nagakubo, K. Nakano and T. Yaguchi of Hitachi High-Technologies Corporation for their help with the TEM observation. This work was supported by the Tohoku University GCOE program for "Global Education and Research Center for Earth and Planetary Dynamics", by a Grant-in-Aid for Challenging Exploratory Research from KAKENHI (25610068) and by the Consolider Project "Factoría de Cristalización" (CSD2006-00015) of the Spanish MINECO.

## ■ REFERENCES


(1) Kelton, K. F.; Greer, A. L. *Nucleation in Condensed Matter: Applications in Materials and Biology*; Elsevier:: Great Britain, 2010.
(2) Kaschiev, D. *Nucleation. Basic Theory with Applications*; Buttherworth-Heinemann:: Oxford, 2000.
(3) Mullin, J. W. *Crystallization*, 3rd ed.; Butterworth-Heinemann:: Oxford, 1993.
(4) Gebauer, D.; Volkel, A.; Colfen, H. *Science* **2008**, *322*, 1819−1822.
(5) Dey, A.; Bomans, P. H. H.; Muller, F. A.; Will, J.; Frederik, P. M.; de With, G.; Sommerdijk, N. A. J. M. *Nat. Mater.* **2010**, *9*, 1010−1014.
(6) Vekilov, P. G. *Cryst. Growth Des.* **2010**, *10*, 5007−5019.
(7) Yau, S. T.; Vekilov, P. G. *J. Am. Chem. Soc.* **2001**, *123*, 1080−1089.
(8) Pouget, E. M.; Bomans, P. H. H.; Goos, J. A. C. M.; Frederik, P. M.; de With, G.; Smmerdijk, N. A. J. M. *Science* **2009**, *323*, 1455−1458.
(9) Van Driessche, A. E. S.; Benning, L. G.; Rodriguez-Blanco, J. D.; Ossorio, M.; Bots, P.; García-Ruiz, J. M. *Science* **2012**, *336*, 69−72.
(10) Yuk, J. M.; Park, J.; Ercius, P.; Kim, K.; Hellebusch, D. J.; Cromie, M. F.; Lee, J. Y.; Zettl, A.; Alivisatos, A. P. *Science* **2012**, *336*, 61−64.
(11) Li, D.; Nielsen, M. H.; Lee, J. R. I.; Frandsen, C.; Banfield, J. F.; de Yoreo, J. J. *Science* **2012**, *336*, 1014−1018.
(12) Liao, H.-G.; Cui, L.; Whitelam, S.; Zheng, H. *Science* **2012**, *336*, 1011−1014.
(13) ten Wolde, P. R.; Frenkel, D. *Science* **1997**, *277*, 1975−1978.
(14) Nicolis, G.; Nicolis, C. *Physica A* **2003**, *323*, 139−154.
(15) Rogers, R. D.; Seddon, K. R. *Science* **2003**, *302*, 792−793.
(16) Arimoto, S.; Sugimura, M.; Kageyama, H.; Torimoto, T.; Kuwabata, S. *Electrochim. Acta* **2008**, *53*, 6228−6234.
(17) Itho, H.; Naka, K.; Chujo, Y. *J. Am. Chem. Soc.* **2004**, *126*, 3026−3027.
(18) Vailati, A.; Cerbino, R.; Mazzoni, S.; Takacs, C. J.; Cannell, D. S.; Giglio, M. *Nat. Commun.* **2011**, *2*, No. 290.
(19) Bennema, P. *J. Cryst. Growth* **1967**, *1*, 287−292.
(20) Davey, R. J.; Schroeder, S. L.; ter Horst, J. H. *Angew. Chem.* **2013**, *52*, 2−16.
(21) Chattopadhyay, S.; Erdemir, D.; Evans, J. M. B.; Ilavsky, J.; Amenitsch, H.; Segre, C. U.; Myerson, A. S. *Cryst. Growth Des.* **2005**, *5*, 523−527.
(22) Niinomi, H.; Yamazaki, T.; Harada, S.; Ujihara, T.; Miura, H.; Kimura, Y.; Kuribayashi, T.; Uwaha, M.; Tsukamoto, K. *Cryst. Growth Des.* **2013**, *13*, 5188−5192.
(23) Ostwald, W. Z. *Phys. Chem.* **1897**, *22*, 289−330.
(24) García-Ruiz, J. M.; Amorós, J. L. *Estud. Geol.* **1980**, *36*, 193−200.
(25) Navrotsky, A. *Proc. Natl. Acad. Sci. U.S.A.* **2004**, *101*, 12096−12101.